Switched sliding-mode control for ZCS series-resonant AC/DC converter

G.-W. Moon
Y.-S. Jung
M.-J. Youn

Indexing terms: Buck–boost converter, Voltage regulation

Abstract: A combined buck and boost zero-current-switched series-resonant AC/DC converter for DC output voltage regulation with a high power factor is proposed. The proposed single-phase AC/DC converter enables a zero-current switching operation of all the power devices, allowing the circuit to operate at high switching frequencies and high power levels. A dynamic model for this AC/DC converter is developed in a discrete-time domain and an analysis for the internal operational characteristics is explored. Based on this analysis, a switched sliding-mode control technique is investigated with its advantages over the other type of current-control technique are discussed. With the proposed control techniques, unity power factor without current overshoot and a wide output voltage range can be obtained.

1 Introduction

To obtain high-quality AC power lines and meet EMI requirements it is necessary for many power electronic equipments to improve the waveform quality of the AC/DC conversion. Recently, there has been a great deal of research on the wave shaping of the active line current by way of hard switching. This type of approach for the line condition, however, has many problems, such as the high switching losses and high EMI level owing to the hard switching [1–4]. To reduce these problems, the resonant converter concepts are promising, as they eliminate the switching losses to such a great extent that the switching frequency can be increased and the level of EMI reduced [5–8]. Among the aforementioned approaches for power factor correction and output voltage regulation, the boost type is the most popular configuration [8]. The boost converter has the advantage of a continuous inductor current in AC line that can be controlled to get an unity power factor. However, there exists an inherent disadvantage like the existence of uncontrollable range when the output voltage is below the peak value of the source voltage. This results in the start-up inrush current as well as overload current. Ultimately, the inductor and the isolation transformer will be saturated and components will fail. Thus much higher ratings of the switching device are required for safe operation. To overcome this disadvantage, the buck operation should be employed for improved control performance and system design optimisation during the start-up transient periods and load fault conditions. Although the buck converter has the characteristics of degrading the input power factor because of the chopped input current [9], it can limit the start-up inrush current and overload current. Thus the buck operation is very useful for safe operation and extending the output voltage range below the peak value of the source voltage. In this paper, it is considered that the fast transient response without overload current and start-up inrush current can be made available by fully utilising both buck and boost operations.

Recently the sliding-mode control (SMC) technique for resonant power switching supply has been introduced in several papers [10–15]. An interesting control technique using the sliding mode in the continuous time domain has been reported [14]. However, since the full state feedback loop is simultaneously analysed with this technique, the analysis is more complex and the existence condition of the sliding regime has not been analytically proven. It is also difficult to design a control law considering the characteristics of each state. To design a sliding-mode controller in the continuous-time domain, an approximated model under several assumptions has been developed. In this paper, the switched SMC in the discrete-time domain is proposed to control the resonant current. Using the proposed switched SMC technique, a unity power factor, better control performance of the DC output voltage regulation over a wide range, and reduced overload and start-up inrush currents are obtained.

2 Basic operation and problem statement

2.1 Principles of basic operation

The basic configuration of a ZCS series-resonant AC/DC converter shown in Fig. 1 consists of a diode bridge rectifier with a high-frequency LC input filter, a full-bridge resonant power stage, a single-switch boost chopper, and an output filter stage. The resonant power stage has two useful operational modes: the powering and freewheeling modes [17]. As shown in Fig. 1, a chopper switch S is added to obtain a boost operation. Note that the changing instants for the operational modes of the resonant power stage and the switching status of S are only allowed at zero-crossing instants of the resonant current.

Paper 2117B (P1), first received 13th December 1994 and in revised form 13th June 1995

The authors are with the Department of Electrical Engineering, Korea Advanced Institute of Science & Technology, 373-1, Kusong-Dong, Yusong-Gu, Taejon, 305-701, Korea

2.1.1 Buck operation: If a chopper switch S is always open, the proposed converter can be classified as a buck converter. In this case the amplitude of the resonant

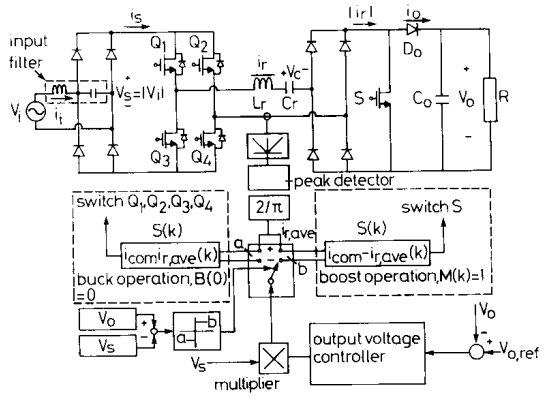

Fig. 1 *Circuit diagram of switched sliding-mode controlled ZCS series resonant AC/DC converter*

current can be controlled according to the operational mode pattern of the resonant power stage. The DC voltage transfer ratio D can be determined as follows:

$$D(p, f) = \frac{p}{p+f} < 1 \tag{1}$$

where p and f denote the number of powering and free-wheeling modes, respectively. Since the DC voltage transfer ratio is less than the unity, the buck-type operation can be possible with the continuous off status of the chopper switch S. The detailed operational principles and an equivalent circuit for each mode are shown in Figs. 2 and 3. Fig. 2 shows that the applied rectified line voltage V_s to the resonant tank circuit is in phase with the resonant current during the powering mode. Thus the resonant current is increased by using the powering mode and is equal to the input current i_s. Fig. 3 shows a detailed operational principle and an equivalent circuit for the free-wheeling mode. The zero voltage is applied to the resonant tank circuit. Thus the amplitude of the resonant current is decreased and the input current i_s becomes zero. The characteristics of the buck operation are summarised in Table 1.

2.1.2 Boost operation: The operation of the ZCS series-resonant AC/DC converter with the boost characteristics can be easily obtained by using the chopper switch S. The switch pairs Q_1, Q_4 and Q_2, Q_3 are always turned on and off alternately at zero-crossing points of the resonant current. The rectified line voltage V_s to the resonant tank circuit is always in phase with the resonant current. Thus the resonant power stage is continuously energised by the rectified line voltage V_s and the input current i_s is

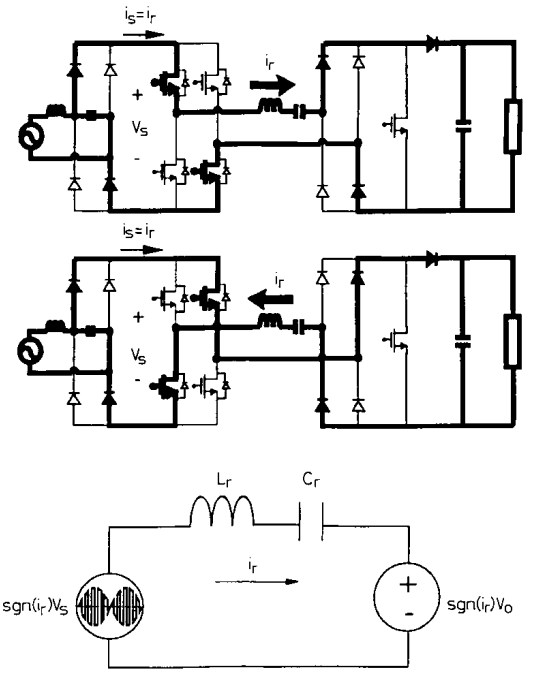

Fig. 2 *Equivalent circuit for buck operation: powering mode, $M(k) = 1$*

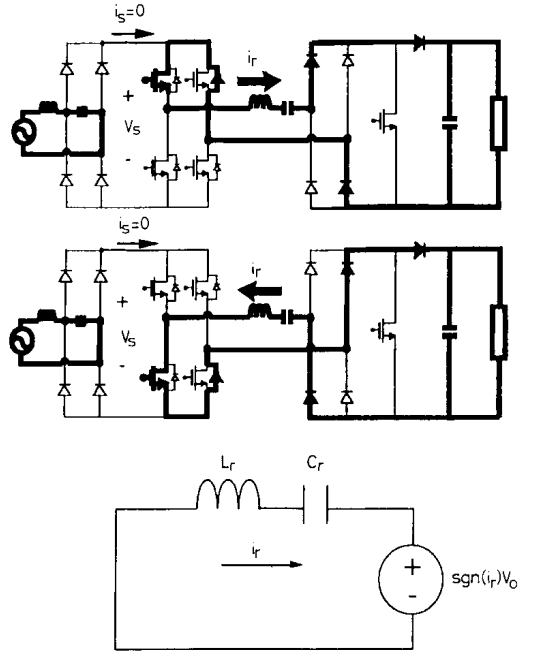

Fig. 3 *Equivalent circuit for buck operation: free-wheeling mode, $M(k) = 0$*

Table 1: Characteristics of buck operation

Basic operational mode		Applied rectified line voltage to tank circuit	Switching status of resonant power stage	Switching status of chopper switch S
Mode	Notation $M(k)$			
powering	1	sgn $(i_r(t))V_s(t)$	$i_r > 0$: Q_1 and Q_4 on $i_r < 0$: Q_2 and Q_3 on	always off
freewheeling	0	0	$i_r > 0$: Q_1 on $i_r < 0$: Q_3 on	$B(k) = 0$

equal to the resonant current i_r. The DC voltage transfer ratio D in this case can be determined as follows:

$$D(k, b) = 1 + \frac{b}{k} > 1 \tag{2}$$

where k and b denote the number of off and on states of the chopper switch S, respectively. Since the DC voltage transfer ratio is greater than the unity, the boost-type operation is possible with the continuous powering mode. Using the continuous powering mode in the resonant power stage, the amplitude of the input and resonant current can be rapidly increased with a maximum slop when the switch S is closed (Fig. 4). If the switch S is

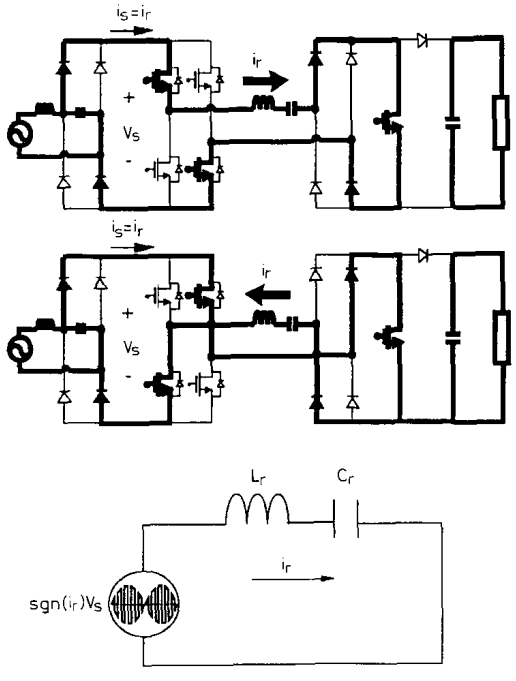

Fig. 4 *Equivalent circuit for boost operation: switching status* $B(k) = 1$

open, as in Fig. 5, the output stage is connected in series with the resonant tank circuit and hence the stored energy in the resonant power stage is transferred to the output stage. In the steady state, the output voltage is generally much greater than the rectified line voltage V_s in the boost operation. Thus the amplitude of the input and resonant current is decreased when the chopper switch S is open. The characteristics of the boost operation are summarised in Table 2.

2.2 Problem statement

The boost-type ZCS series-resonant AC/DC converter has many advantages over the conventional boost-type PWM converters, such as the zero switching loss, smaller

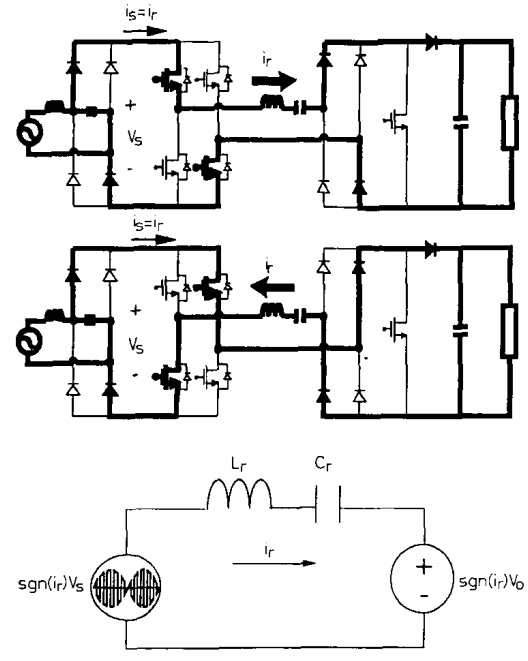

Fig. 5 *Equivalent circuit for boost operation: switching status* $B(k) = 0$

filter size, and lower EMI levels, etc. Also, it shows that the steady-state peak current level is much smaller than that of a buck-type ZCS series-resonant AC/DC converter. However, the boost topology is basically employed only when the output voltage is greater than the peak value of the rectified line voltage. If a load fault condition occurs, the output voltage will be dragged down below the peak value of the rectified line voltage. When this occurs, the current will rise rapidly without limit. Since the current rises above a desirable level, the chopper switch S is held off by the control circuit. Therefore the boost-type converter cannot control the current reduction. Furthermore, since the output voltage is zero during the start-up transients, start-up inrush current and output voltage overshoot also occur. Thus the boost-type AC/DC converter has uncontrollable range during the load fault condition and start-up transient period. Although the proposed converter is complex and has a discontinuous input current to utilise the buck operation, a wide range of output voltage without a large current

Table 2: Characteristics of boost operation

Switching status of chopper switch S		Reflected output voltage to tank circuit	Switching status of resonant power stage
Status	Notation $B(k)$		
On	1	0	always
off	0	sgn $(i_r(t))V_o(t)$	powering mode $i_r > 0$: Q_1 and Q_4 on $i_r < 0$: Q_2 and Q_3 on

overshoot is available by fully utilising both buck and boost operations.

3 Dynamic modelling

To obtain a simple and effective analysis, a dynamic model in the discrete-time domain is developed. Since both the changes of the operational modes in the resonant power stage and switching status of chopper switch S can be affected at any control instant, the control variables representing these control inputs for the kth time event are defined as $M(k)$ and $B(k)$, respectively. The control variable $M(k)$ has the values of 1 and 0 denoting the powering and freewheeling modes in the resonant power stage for the kth time event, respectively. Also $B(k)$ has the values of 1 and 0 expressing the on and off status of S for the kth time event, respectively. Based on the basic operational principles, the governing equations for the proposed AC/DC converter can be derived as follows:

$$\text{sgn}\,(i_r(t))M(k)V_s(t) = L_r\frac{di_r(t)}{dt} + v_c(t) + (1 - B(k))\,\text{sgn}\,(i_r(t))V_o(t) \quad (3)$$

$$C_r\frac{dv_c(t)}{dt} = i_r(t) \quad (4)$$

$$(1 - B(k))\,|i_r(t)| = C_o\frac{dV_o(t)}{dt} + \frac{1}{R_L}V_o(t) \quad (5)$$

The left-hand side of eqn. 3 implies the actual applied rectified line voltage to the resonant power state with respect to the operational mode, the third term of the right-hand side denotes the output voltage reflected to the resonant power stage. Eqn. 4 refers to the dynamic behaviour between the resonant capacitor voltage and resonant inductor current. The output equation with respect to the switching status of switch S can be expressed as in eqn. 5. Because the rectified line voltage V_s and output voltage V_o during the half resonant interval can be assumed as constants by the low-ripple approximation [17], the absolute resonant current can be derived from eqns. 3 and 5 as follows:

$$|i_r(t)| = \frac{v_c^*(k) + M(k)V_s(k) - (1 - B(k))V_o(k)}{Z} \times \sin\{\omega_r(t - kT/2)\} \quad \text{for } \frac{kT}{2} \leqslant t \leqslant \frac{(k+1)T}{2} \quad (6)$$

where $z = \sqrt{(L_r/C_r)}$, $T = 2\pi\sqrt{(L_r/C_r)}$, $\omega_r = 1/\sqrt{(L_r/C_r)}$, and $v_c^*(k)$ is defined as the absolute value of $v_c(k)$. From eqns. 3–6, the following equation can also be easily obtained:

$$v_c^*(k+1) = \frac{1}{C_r Z}\int_{kT/2}^{(k+1)T/2}\{v_c^*(k) + M(k)V_s(k) - (1 - B(k))V_o(k)\} \times \sin\left\{\omega_r\left(t - \frac{kT}{2}\right)\right\}dt - v_c^*(k) \quad (7)$$

$$V_o(k+1) = \frac{1}{C_o Z}\int_{kT/2}^{(k+1)T/2}\{v_c^*(k) + M(k)V_s(k) - (1 - B(k))V_o(k)\}\sin\left\{\omega_r\left(t - \frac{kT}{2}\right)\right\}dt + V_o(k) - \frac{1}{C_o}\int_{kT/2}^{(k+1)T/2}\frac{V_o(k)}{R_L}dt \quad (8)$$

If a new discrete state variable is defined as $i_{r,\,ave}(k)$ representing the average value of the absolute resonant current during the kth time event, the following equation can be obtained from eqn. 6:

$$i_{r,\,ave}(k) \equiv \frac{2}{\pi}|i_{r,\,p}(t)| = \frac{2}{\pi}\frac{v_c^*(k) + M(k)V_s(k) - (1 - B(k))V_o(k)}{Z} \quad \text{for } \frac{kT}{2} \leqslant t < \frac{(k+1)T}{2} \quad (9)$$

where $|i_{r,\,p}(k)|$ denotes the absolute peak value of the resonant current during the kth time event. Solving eqns. 7 and 8 gives

$$v_c^*(k+1) = v_c^*(k) + 2M(k)V_s(k) - 2(1 - B(k))V_o(k) \quad (10)$$

$$V_o(k+1) = \gamma(1 - B(k))v_c^*(k) + M(k)V_s(k) + (1 - B(k))V_o(k) + V_o(k) - \gamma^*V_o(k) \quad (11)$$

where $\gamma = 2C_r/C_o$ and $\gamma^* = \pi Z\gamma/(2R_L)$. The average value of the absolute resonant current for the $(k+1)$th time event can also be obtained by simply replacing the time index k of eqn. 9 by $(k+1)$ as

$$i_{r,\,ave}(k+1) = \frac{2}{\pi}\frac{v_c^*(k+1) + M(k+1)V_s(k+1) - (1 - B(k+1))V_o(k+1)}{Z} \quad (12)$$

Using eqns. 9–12, the following discrete state equation for a buck and boost combined ZCS series-resonant AC/DC converter can be derived as

$$\begin{pmatrix} i_{s,\,ave}(k+1) \\ v_o(k+1) \end{pmatrix} = \begin{pmatrix} 1 - \gamma(1 - S(k))(1 - S(k+1)) & \frac{\pi Z\gamma}{2}(1 - S(k)) \\ -\frac{2}{\pi Z}(1 - S(k)) + (1 - \gamma^*)(1 - S(k+1)) & 1 - \gamma^* \end{pmatrix} \times \begin{pmatrix} i_{r,\,ave}(k) \\ V_o(k) \end{pmatrix} + \begin{pmatrix} \frac{4V_s(k)}{\pi Z} \\ 0 \end{pmatrix}\frac{M(k) + M(k+1)}{2} \quad (13)$$

Since C_r is chosen much smaller than C_o, γ and γ^* become much smaller than unity. Therefore, eqn. 13 can

be simplified as follows:

$$\begin{pmatrix} i_{r,\,ave}(k+1) \\ V_o(k+1) \end{pmatrix} = \begin{pmatrix} 1 & -\dfrac{4}{\pi Z}(1 - S^*(k+1)) \\ \dfrac{\pi Z\gamma}{2}(1 - S(k)) & 1 - \gamma^* \end{pmatrix} \times \begin{pmatrix} i_{r,\,ave}(k) \\ V_o(k) \end{pmatrix} + \begin{pmatrix} \dfrac{4v_s(k)}{\pi Z} \\ 0 \end{pmatrix} + \begin{pmatrix} \dfrac{4V_s(k)}{\pi Z} \\ 0 \end{pmatrix} M^*(k+1) \quad (14)$$

where $B^*(k+1)$ and $M^*(k+1)$ are defined, respectively, as

$$B^*(k+1) = \{B(k) + B(k+1)\}/2 \quad (15)$$

$$M^*(k+1) = \{M(k) + M(k+1)\}/2 \quad (16)$$

If $B(k)$ is set to zero for all k, that is the switch S is open, this equation can be reduced to a dynamic model for a buck ZCS series-resonant AC/DC converter. In this case $M(k)$ becomes a control variable. On the other hand, if $M(k)$ is always set to unity for all k, that is the resonant power stage is always operated in the powering mode, a boost ZCS series-resonant AC/DC converter can be modelled. In this case $B(k)$ becomes a control variable. Note that the average values of the absolute resonant current $i_{r,\,ave}(k+1)$ are directly controlled by $B^*(k+1)$ in case of the boost operation and directly controlled by $M^*(k+1)$ in case of the buck operation. The dynamic model and current slope equation, slope$(k, k+1)$, for the buck and boost ZCS series-resonant AC/DC converter can be easily derived from eqn. 14 as follows:

Buck ZCS series-resonant AC/DC converter

$$\begin{pmatrix} i_{r,\,ave}(k+1) \\ V_o(k+1) \end{pmatrix} = \begin{pmatrix} 1 & -\dfrac{4}{\pi Z} \\ \dfrac{\pi Z\gamma}{2} & 1 - \gamma^* \end{pmatrix} \begin{pmatrix} i_{r,\,ave}(k) \\ V_o(k) \end{pmatrix} + \begin{pmatrix} \dfrac{4V_s(k)}{\pi Z} \\ 0 \end{pmatrix} M^*(k+1) \quad (17)$$

$$\text{slope}\,(k, k+1) = \frac{i_{r,\,ave}(k+1) - i_{r,\,ave}(k)}{(T/2)} = \frac{8}{\pi ZT}\{M^*(k+1)V_s(k) - V_o(k)\} = \frac{1}{L_{eq}}\{M^*(k+1)V_s(k) - V_o(k)\}$$

where

$$L_{eq} = \left(\frac{\pi}{2}\right)^2 L_r \quad (18)$$

Boost ZCS series-resonant AC/DC converter

$$\begin{pmatrix} i_{r,\,ave}(k+1) \\ V_o(k+1) \end{pmatrix} = \begin{pmatrix} 1 & -\dfrac{4}{\pi Z}(1 - B^*(k+1)) \\ \dfrac{\pi Z\gamma}{2}(1 - B(k)) & 1 - \gamma^* \end{pmatrix} \times \begin{pmatrix} i_{r,\,ave}(k) \\ V_o(k) \end{pmatrix} + \begin{pmatrix} \dfrac{4V_s(k)}{\pi Z} \\ 0 \end{pmatrix} \quad (19)$$

$$\text{slope}\,(k, k+1) = \frac{i_{r,\,ave}(k+1) - i_{r,\,ave}(k)}{(T/2)} = \frac{8}{\pi ZT}\{V_s(k) - (1 - B^*(k+1))V_o(k)\} = \frac{1}{L_{eq}}\{V_s(k) - (1 - B^*(k+1))V_o(k)\} \quad (20)$$

Note that the behaviour of $i_{r,\,ave}(k+1)$ is controlled by both $M^*(k+1)$ and $B^*(k+1)$. Since three values are possible for each $M^*(k+1)$ and $B^*(k+1)$, three kinds of current slopes are available for the proposed converter.

4 Switched sliding-mode control technique and analysis

In this Section, a switched sliding-mode control (SSMC) technique is developed and its advantages over the other types of current control technique are compared. The main control objectives for the AC/DC converter are to shape the line current into a sinewave keeping in phase with the line voltage without large current overshoot and also to obtain a desirable control performance for output voltage regulation. The boost-type converter is often used to satisfy these control objectives owing to the advantage of continuous line current. However, there exists an inherent disadvantage such as the uncontrollable range during the start-up transient period and load fault condition. Fig. 6 shows the typical start-up transient response for the boost operation. The uncontrollable ranges exist when $V_o(k)$ smaller than $V_s(k)$. Since $M^*(k+1)$ is always set to the unity in a boost ZCS series-resonant AC/DC converter, the current slope is always positive for any value of $B^*(k+1)$ in the range of $V_o(k)$ smaller than $V_s(k)$.

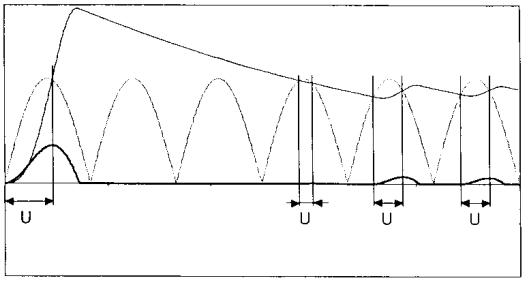

Fig. 6 *Typical start-up transient response: bang-bang boost type*
——— rectified line current i_s
····· rectified line voltage V_s
——— output voltage V_o
U = uncontrollable range, $V_o < V_s$

Hence, the resonant current cannot be properly controlled until $V_o(k)$ becomes greater than $V_s(k)$, and the start-up inrush current appears during the transient period.

To deal with this problem, it is considered that a buck operational mode should be properly used in the range of $V_o(k)$ smaller than $V_s(k)$ to eliminate the uncontrollable range, and then a boost operation is employed above the range. This basic strategy for the elimination of the uncontrollable ranges is shown in Fig. 7b. By properly choosing the operational-mode patterns in the range of $V_o(k)$ smaller than $V_s(k)$, a sliding-mode control technique for the buck ZCS series-resonant AC/DC converter can be employed. This control concept is further extended to a boost operation for the range of $V_o(k)$ greater than $V_s(k)$ to obtain unity power factor.

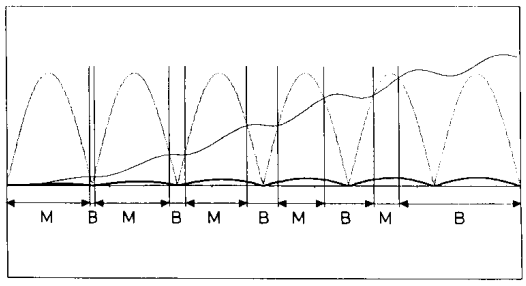

Fig. 7 *Typical start-up transient response: switched sliding-mode control technique*

——— rectified line current i_s
····· rectified line voltage V_s
——— output voltage V_o
M = buck operation, $V_o < V_s$
B = boost operation, $V_o > V_s$

4.1 Buck operation

4.1.1 Switching strategy: Based on the discrete sliding-mode control (DSMC) the strategy in the case of the buck operation is expressed as follows:

$$M(k+1) = 1 \quad \text{for } S(k) > 0 \tag{21}$$

$$M(k+1) = 0 \quad \text{for } S(k) < 0 \tag{22}$$

where $S(k)$ represents the switching surface in the kth time event. This switching surface consisting of the average value of the absolute resonant current and its command i_{com} in the kth time event is expressed as

$$S(k) = i_{com} - i_{r,ave}(k) \tag{23}$$

When a quasisliding-mode exists on $S(k) = 0$, the average motion of the system response is determined by the smooth control function called the equivalent operational mode. In the discrete-time domain, the equivalent operational mode $M^*_{eq}(k+1)$ is obtained from eqns. 17 and 23, and the forward difference of the switching surface is

$$S(k+1) - S(k) = 0 \tag{24}$$

$$M^*_{eq}(k+1) = \frac{V_o(k)}{V_s(k)} \tag{25}$$

The eqn. 25 shows that the equivalent operational mode coincides with the duty ratio between the rectified line voltage and the output voltage, and also satisfies the following equation in case of the buck-type converter:

$$0 < M^*_{eq}(k+1) < 1 \tag{26}$$

This equation implies that the proper operational mode can always be generated when the output voltage is smaller than the rectified line voltage. If the equivalent operational mode is employed in eqn. 17 the resonant current dynamics are eliminated. In other words, the dynamic relation between the output voltage and the average value of the absolute resonant current command can be easily obtained using eqn. 20 as

$$V_o(k+1) = (1 - \gamma^*)V_o(k) + \frac{\pi Z \gamma}{2} i_{com} \tag{27}$$

Since eqn. 27 is a first-order model, the various types of the output voltage controller can be easily designed.

4.1.2 Analysis for sliding regime: The existence condition for a sliding mode in the continuous-time domain is

$$\lim_{s \to 0} s \frac{ds}{dt} < 0 \tag{28}$$

where s represents the switching surface. The condition (expr. 28) that ensures the sliding motion on the switching surface in a continuous system is no longer applicable to the proposed discrete-time domain model. Thus an intuitively obvious definition of sliding motion in the discrete-time domain was proposed in [16]. For a quasi-sliding motion this is

$$|S(k+1)| < |S(k)| \tag{29}$$

If expr. 29 is decomposed into two inequalities it becomes

$$(S(k+1) - S(k)) \operatorname{sgn}(S(k)) < 0 \tag{30}$$

$$(S(k+1) + S(k)) \operatorname{sgn}(S(k)) > 0 \tag{31}$$

Expr. 30 assures the quasisliding motion on the switching surface, and the convergence of the state trajectories on the switching surface is assured by expr. 31. In the following discussion the detailed analysis for the sliding condition (expr. 30) is examined for the proposed buck-type AC/DC converter, which is modelled in the discrete form. Using the current slope equation (eqn. 18), expr. 30 can be expressed as

$$\begin{aligned}(S(k+1) - S(k)) \operatorname{sgn}(S(k)) &= \frac{4}{\pi Z} \operatorname{sgn}(S(k))[M^*(k+1)V_s(k) - V_o(k)] \\ &= \frac{4}{\pi Z}\left(\frac{T}{2}\right) \operatorname{sgn}(S(k))\, slope\,(k, k+1) < 0\end{aligned} \tag{32}$$

The slope of the average value of absolute resonant current must be positive to satisfy the sliding condition in the regions of $S(k) > 0$, that is, slope $(k, k+1) > 0$. On the other hand, the negative current slope is needed to assure the sliding condition in the regions of $S(k) < 0$, that is slope $(k, k+1) < 0$. It is obvious that the state is moved toward the switching surface $S(k) = 0$. In other words, the average value of the resonant current directly follows the current command. The current slope is controlled by the moving average value of the operational mode. Since three values are possible for $M^*(k+1)$ as seen in eqn. 18, three kinds of conditions are available for each positive and negative current slope. The possible conditions for the current slope with respect to $M^*(k+1)$ are summarised in Table 3. However, the condition $M^*(k+1) = 0$ does not occur because $M(k+1)$ is always unity by the switching strategy (expr. 21) in the regions of $S(k) > 0$. Similarly, the case of $M^*(k+1) = 1$

Table 3: Current slope analysis for buck operation

$M^*(k+1)$	Slope $(k, k+1)$	Positive current slope condition	Negative current slope condition
0	$\frac{1}{L_{eq}}[-V_o(k)]$	$-V_o(k) > 0$	$-V_o(k) < 0$
		none	always
0.5	$\frac{1}{L_{eq}}[\frac{1}{2}V_s(k) - V_o(k)]$	$V_s(k) > 2V_o(k)$	$V_s(k) < 2V_o(k)$
1	$\frac{1}{L_{eq}}[V_s(k) - V_o(k)]$	$V_s(k) > V_o(k)$	$V_s(k) < V_o(k)$
		always	none

for the negative slope condition is not available because $M(k+1)$ always has a zero value by the switching strategy (expr. 22) in the regions of $S(k) < 0$. The conditions $V_s(k) > V_o(k)$ when $M^*(k+1) = 1$, and $-V_o(k) < 0$ when $M^*(k+1) = 0$, are always satisfied in buck operation. Thus the only interesting condition is confined to the case of $M^*(k+1) = 0.5$ which comes from the change in operational modes. For example, if $M(k) = 0$ for the positive slope condition, the next operational mode is set to unity $M(k+1) = 1$ by the switching strategy of expr. 21, and if $M(k) = 1$ the next operational mode has a zero value $M(k+1) = 0$ by the switching strategy of expr. 22. In this case $M^*(k+1) = 0.5$, the negative current slope is only available under the condition of $V_s(k) < 2V_o(k)$ as seen in Table 3. Therefore the sliding regime is assured in the region of $S(k) < 0$ in which only the negative current slope is needed to confirm the sliding condition (expr. 30). However, the sliding condition is not satisfied in the region of $S(k) > 0$ in which the positive current slope is needed to confirm the sliding condition. Although the sliding condition is relaxed during the transient periods of the operational mode under the conditions of $V_s(k) < 2V_o(k)$ for $S(k) > 0$ and $V_s(k) > 2V_o(k)$ for $S(k) < 0$, the sliding condition is at least satisfied after the finite sampling time. In other words, the prediction of the sliding surface is expected to have negative values, which is equivalent to having a positive current slope, or V_s is larger than $2V_o$. This analysis is summarised in the following lemma 1.

Lemma 1 (modified sliding condition): For the proposed buck-type AC/DC converter (eqn. 17), the sliding condition for the existence of a quasisliding regime is at least satisfied after the finite N sampling time. This can be expressed as follows:

$$[S(k+N) - S(k)] \text{ sgn } (S(k)) < 0 \quad \text{for } \forall k \tag{33}$$

The proof of lemma 1 is presented in the Appendix.

4.2 Boost operation

4.2.1 Switching strategy: The strategy based on the DSMC in the case of boost operation is

$$B(k+1) = 1 \quad \text{for } S(k) > 0 \tag{34}$$

$$B(k+1) = 0 \quad \text{for } S(k) < 0 \tag{35}$$

The switching surface consisting of the average value of the resonant current and its command i_{com} is as follows:

$$S(k) = i_{com} - i_{r,ave}(k) \tag{36}$$

In a similar way to buck operation, the equivalent control signal for S is derived from exprs. 19 and 31 as

$$B^*_{eq}(k+1) = 1 - \frac{V_s(k)}{V_o(k)} \tag{37}$$

Eqn. 37 shows that the equivalent control signal for S coincides with the duty ratio between input voltage and output voltage, and also satisfies the following equation in the case of the boost-type converter as

$$0 < B^*(k+1) < 1 \tag{38}$$

This equation implies that the control signal for S can always be generated when the rectified line voltage is smaller than the output voltage.

4.2.2 Analysis for sliding regime: In the following discussion, detailed analysis for the sliding condition of expr. 30 is examined for the proposed boost-type AC/DC converter, which is modelled in discrete form. Using the current slope equation (eqn. 20), expr. 30 can be expressed as

$$\begin{aligned}(S(k+1) - S(k)) \text{ sgn } (S(k)) &= -\frac{4}{\pi Z} \text{ sgn } (S(k))[V_s(k) - (1 - B^*(k+1))V_o(k)] \\ &= -\frac{4}{\pi Z}\left(\frac{T}{2}\right) \text{ sgn } (S(k)) \text{ slope } (k, k+1) < 0\end{aligned} \tag{39}$$

The slope of the average resonant current must be positive to satisfy the sliding condition in the regions of $S(k) > 0$, that is slope $(k, k+1) > 0$. On the other hand, the negative current slope is needed to assure the sliding condition in the regions of $S(k) < 0$, that is slope $(k, k+1) < 0$. It is clear that the state is moved toward the switching surface. In other words, the average resonant current directly follows the current command. Note that the current slope is controlled by the moving average value of the operational mode or the switching signal for B. Since three values are possible for $B^*(k+1)$, three kinds of conditions are available for each positive and negative current slope. The possible conditions for the current slope with respect to $B^*(k+1)$ are summarised in Table 4. The condition $B^*(k+1) = 0$ does not occur because $B(k+1)$ is always unity by the switching strategy of expr. 34 in the region of $S(k) > 0$. Similarly, the case of $B^*(k+1) = 1$ for the negative slope condition is not available because $B(k+1)$ always has zero value by the switching strategy of expr. 35 in the region of $S(k) < 0$.

The conditions $V_s(k) < V_o(k)$ when $M^*(k+1) = 0$ and $V_s(k) > 0$ when $M^*(k+1) = 1$ are always satisfied in boost operation. Thus, the only interesting condition is confined to the case of $B^*(k+1) = 0.5$ which comes from the change of the control signal for S. For example, if $B(k) = 0$, the next control signal for S is set to the unity $B(k+1) = 1$ by the switching strategy of expr. 34, and if $B(k) = 1$ the next control signal for S has a zero value $B(k+1) = 0$ by the switching strategy of expr 35. In the case of $B^*(k+1) = 0.5$, the negative current slope is only available under the condition of $V_s(k) < V_o(k)/2$, as seen in Table 4. Therefore the sliding regime is assured in the

Table 4: Current slope analysis for boost operation

$B^*(k+1)$	Slope $(k, k+1)$	Positive current slope condition	Negative current slope condition
0	$\frac{1}{L_{eq}}[V_s(k) - V_o(k)]$	$V_s(k) > V_o(k)$	$V_s(k) < V_o(k)$
		none	always
0.5	$\frac{1}{L_{eq}}[V_s(k) - \frac{1}{2}V_o(k)]$	$V_s(k) > \frac{1}{2}V_o(k)$	$V_s(k) < \frac{1}{2}V_o(k)$
1	$\frac{1}{L_{eq}}[V_s(k)]$	$V_s(k) > 0$	$V_s(k) < 0$
		always	none

region of $S(k) < 0$ in which only the negative current slope is needed to confirm the sliding condition (expr. 30). However, the sliding condition is violated in the region of $S(k) > 0$ in which the positive current slope is needed to confirm the sliding condition. Although the condition is relaxed during the transient periods of the control signal for S under the conditions of $V_s(k) < V_o(k)/2$ for $S(k) > 0$ and $V_s(k) > V_o(k)/2$ for $S(k) < 0$, the sliding condition is at least satisfied after the finite sampling time. In other words, the prediction of the sliding surface is expected to have negative values, which is equivalent to a positive current slope, or V_s is larger than $V_o/2$. This analysis is summarised in lemma 2.

Lemma 2 (modified sliding condition): For the proposed boost-type AC/DC converter (eqn. 19), the sliding condition for the existence of a quasisliding regime is at least satisfied after finite N sampling time. This can be expressed as follows:

$$[S(k+N) - S(k)]\ \text{sgn}\ (S(k)) < 0 \quad \text{for } \forall k \tag{40}$$

Since the proof of lemma 2 is very similar to that of lemma 1 it is omitted.

5 Simulations and experimental verification

The advantages of the proposed control technique are comparatively simulated with the bang-bang boost-type current control technique shown in Figs. 9–15. The parameters used are $V_i = 100\ V_{rms}$; $C_o = 800\ \mu F$; $R = 50\ \Omega$; $L_r = 500\ \mu H$, resonant frequency = 100 kHz. The block diagram of bang-bang boost-type current control technique is shown in Fig. 8. The major advantage of this is the simple implementation since only boost

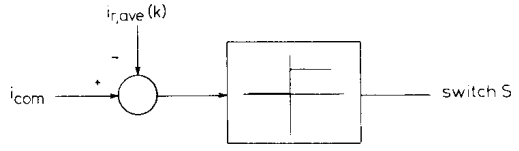

Fig. 8 *Block diagram of bang-bang boost type control technique*

operation is used. However, the control performances are generally shown to be undesirable during the startup transient period and load fault condition. As seen in Fig. 1, the proposed scheme employs the switching technique of the buck and boost operation to improve the control performance. With this strategy, the steady-state responses for the arbitrary current commands are simulated. Since only the boost operation is available in the steady state, the responses are the same for the two kinds of control technique. Fig. 9 shows the simulated waveforms of the rectified line voltage, the average value of the rectified line current and the output voltage. The line current shows the sinusoidal waveform keeping in phase with the line voltage. Thus unity power factor can be obtained for both control techniques. For the purpose of comparison, the rectified line voltage, rectified line current, and output voltage of a boost-type ZCS series-

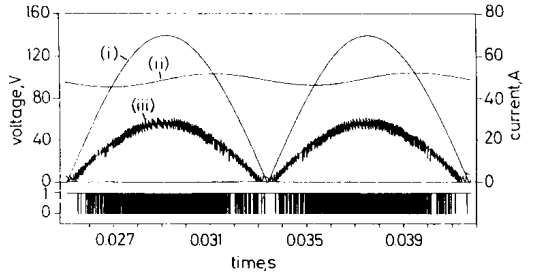

Fig. 9 *Steady-state response for boost and SSMC techniques*
(i) rectified line voltage V_s
(ii) output voltage 3, $V_o/3$
(iii) average value of rectified line current

resonant AC/DC converter using a bang-bang current-control technique are simulated in Fig. 10. It shows the large current overshoot in the first halfcycle and the output voltage response is rapidly increased. As expected, these problems are effectively overcome using the proposed SSMC, as shown in Fig. 11. Since the reduced current overshoot can be obtained, system design optimisation with respect to the ratings of the switching device is possible. The other advantage of the proposed SSMC

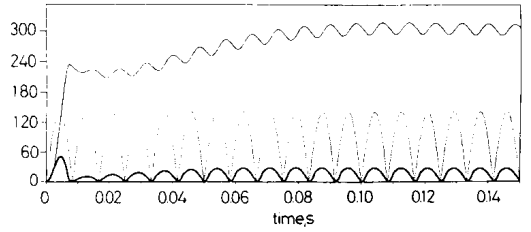

Fig. 10 *Start-up transient response for $V_{o,ref} = 300\ V$: bang-bang boost type*
rectified line current
rectified line voltage
output voltage

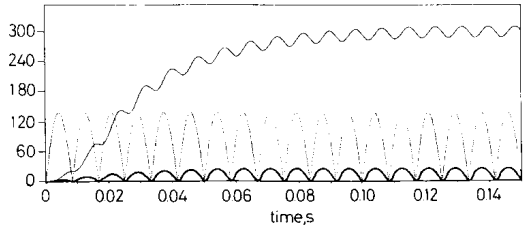

Fig. 11 *Start-up transient response for $V_{o,ref} = 300\ V$: switched sliding-mode control technique*
rectified line current
rectified line voltage
output voltage

technique is that the controllable output voltage ranges are wider than the conventional boost type.

Figs. 12 and 13 show the simulated waveforms when the output voltage reference is 100 V DC which is smaller

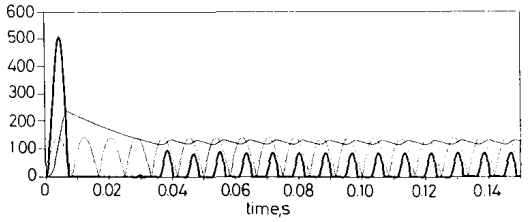

Fig. 12 *Start-up transient response for $V_{o,ref}$ = 100 V: bang-bang boost type*

rectified line current × 10
rectified line voltage
output voltage

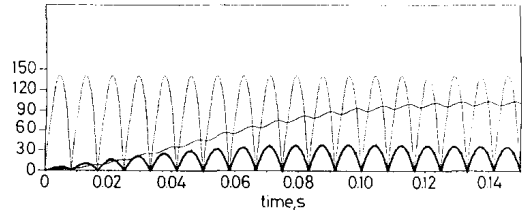

Fig. 13 *Start-up transient response for $V_{o,ref}$ = 100 V: switched sliding-mode control technique*

rectified line current × 10
rectified line voltage
output voltage

than the peak value of the rectified line voltage. As seen in Fig. 12, the start-up inrush current appears during the startup transient and the uncontrollable regions are shown in the steady state. This results in a poor power factor in the range of lower output voltage with undesirable output voltage regulation. However, the responses of the proposed SSMC are desirable in view of the power factor correction and the wide range of output voltage regulation as seen in Fig. 13. If a load fault condition occurs, the output voltage will drop below the peak value of the rectified line voltage and the current will rise rapidly, as seen in Fig. 14. Therefore the inductor and the

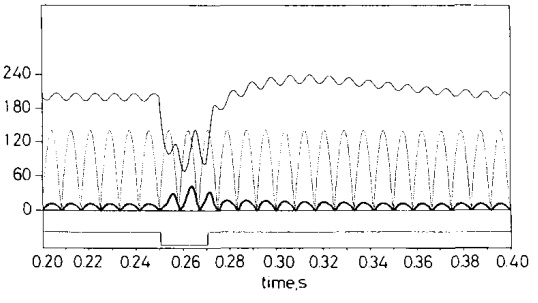

Fig. 14 *Load fault transient response for $V_{o,ref}$ = 200 V: bang-bang boost type*

rectified line current
rectified line voltage
output voltage

isolation transformer will be saturated and the components will fail. Thus much higher ratings of the switching devices are required for safe operation. These problems can be eliminated by the proposed scheme shown in Fig. 15.

The proposed experimental SSMC technique is shown in Figs. 16–19. The parameters used are: $V_i = 100\ V_{rms}$; $V_{o,ref} = 170$ V DC; $C_o = 2200\ \mu$F; $R = 200\ \Omega$; $C_r = 20$ nF; $L_r = 175\ \mu$H; and resonant frequency = 85 kHz.

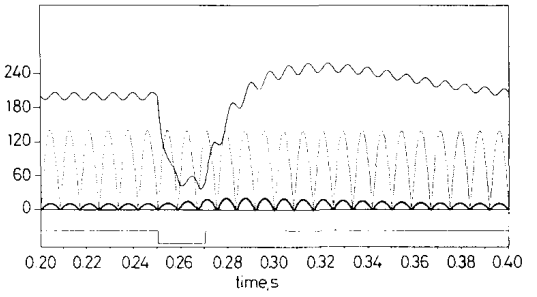

Fig. 15 *Load fault transient response for $V_{o,ref}$ = 200 V: switched sliding-mode control technique*

rectified line current
rectified line voltage
output voltage

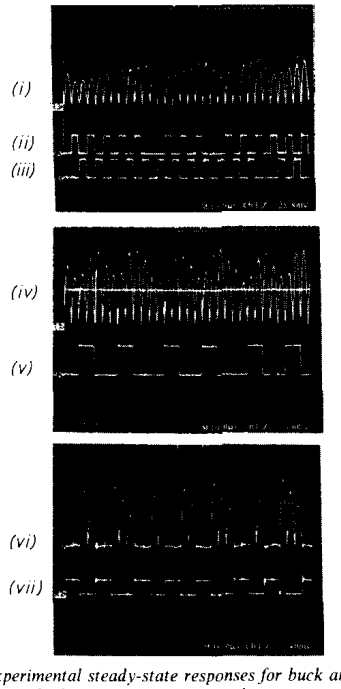

Fig. 16 *Experimental steady-state responses for buck and boost operations in the case of arbitrary current command*

Buck operation:
(i) rectified resonant current $|i_r|$, 5 A/div
(ii) control signal for switch Q_1, 10 V/div, ON = 15 V
(iii) control signal for switch Q_2, 10 V/div, ON = 15 V (powering mode: Q_1 or Q_2 = ON; free-wheeling mode: $Q_1 = Q_2$ = OFF)
Boost operation:
(iv) rectified resonant current $|i_r|$, 2 A/div
(v) control signal for switch S, 10 V/div, ON = 15 V
(vi) output current i_o, 2 A/div
(vii) control signal for switch S, 10 V/div, ON = 15 V

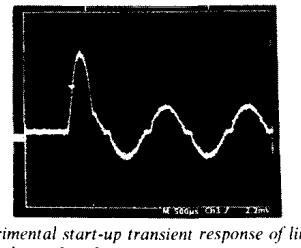

Fig. 17 *Experimental start-up transient response of line current i_1 for bang-bang boost scheme, 2 A/div*

Fig. 16 shows the experimental results for the internal operation of a ZCS series-resonant AC/DC converter. The switching loss is low because the switching instants

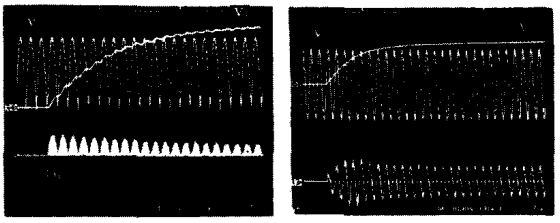

Fig. 18 *Experimental start-up transient responses using proposed controller*
Voltage: 100 V/div; current: 10 A/div

Fig. 19 *Experimental steady-state response using proposed controller*
Voltage: 100 V/div; current: 5 A/div

are synchronised to the zero-current crossing points. Fig. 17 shows the start-up transient response of the line current i_i for the bang-bang boost-type AC/DC converter. The bang-bang boost scheme has uncontrollable range when the output voltage is smaller than the peak value of the rectified line voltage. This results in an inrush during the start-up transient. For the purpose of safe operation, a line voltage V_i of 18 V_{rms} is actually applied in this experiment. The experimental start-up and steady-state responses for the proposed converter are shown in Figs. 18 and 19. The start-up inrush current are reduced remarkably owing to the elimination of the uncontrollable range. Furthermore, the line current i_i closely follows a sinusoidal shape and is in phase with the line voltage V_i during the start-up transient as well as the steady state, resulting in an almost unity power factor.

6 Conclusion

A combined buck and boost zero-current-switched (ZCS) series-resonant AC/DC converter for the DC output voltage regulation together with a high input power factor has been proposed. The proposed single-phase AC/DC converter enabled a zero-current switching operation of all the power devices, allowing the circuit to operate at high switching frequencies and high power levels. A dynamic model for this AC/DC converter has been developed and an analysis for the internal operational characteristics explored. Based on this analysis, a switched sliding-mode control (SSMC) technique was investigated and its advantages over the other types of current control technique discussed. With the proposed control technique, unity power factor as well as a wide ranges of DC output voltage regulation without any inrush current during the start-up transient and load fault condition have been obtained.

7 References

1 MANIAS, S., and ZIOGAS, P.D.: 'An SMR topology with suppressed DC link components and predictive line current wave shaping'. IEEE Industry Application Society Annual Meeting, 1986, pp. 630–639
2 LIU, K.H., and LIN, Y.L.: 'Current waveform distortion in power factor correction circuits employing discontinuous-mode boost converters'. IEEE specialist conference on *Power electronics*, 1989, pp. 825–829
3 KAZERANI, M., ZIOGAS, P.D., and JOOS, G.: 'A novel current waveshaping technique for solid-state input power factor conditioners', *IEEE Trans. Ind. Electron.*, 1991, **IE-38**, (1), pp. 72–78
4 DIXION, L.: 'High power factor switching preregulator design optimization'. Unitrode Switching Regulated Power Supply Design Seminar Manual, 1991, pp. 13-1–13-12
5 SEBASTIAN, J., UCEDA, J., COBOS, J.A., and GIL, P.: 'Using zero-current-switched quasi-resonant converters as power factor preregulator'. IEEE conference on *Industry electronics*, 1991, pp. 225–230
6 DONCKER, R.W., and VENKATARAMANAN, G.: 'A new single phase AC to DC zero voltage soft switching converter'. IEEE Specialist conference on *Power electronics*, 1990, pp. 206–212
7 KHERLUWALA, M.H., STEIGERWALD, R.L., and GURUMOORTHY, R.: 'Performance characterization of a high power factor power supply with a single power stage'. IEEE Industry Application Society Annual Meeting, 1992, pp. 659–665
8 MOON, G.W., JO, B.R., AHN, H.W., and YOUN, M.J.: 'Dynamic modeling and predictive current control technique for ZCS power factor preregulator'. IEEE international symposium of *Industry electronics*, 1993, pp.498–502
9 ENDO, H., YAMASHITA, T., and SUGIURA, T.: 'A high-power-factor buck converter'. IEEE specialist conference on *Power electronics*, 1992, pp. 1071–1076
10 MALESANI, L., ROSSETTO, L., SPIAZZI, G., and TENTI, P.: 'Performance optimization of cuk converter by sliding-mode control'. IEEE conference on *Applied Power electronics*, 1992, pp. 395–402
11 ROSSETTO, L., SPIAZZI, G., and TENTI, P.: 'Fast-response high-quality rectifier with sliding-mode control'. IEEE conference on *Applied power electronics*, 1993, pp. 175–181
12 VENKATARAMANAN, G., and DIVAN, D.M.: 'Discrete time integral sliding mode control for discrete pulse modulated converter'. IEEE specialist conference on *Power electronics*, 1990, pp. 67–73
13 GROEF, A.E., BOSCH, P.P., and VISSER, H.R.: 'Multi-input variable structure controller for electric converter'. European conference on *Power electronics*, 1991, pp. 1-001–1-006
14 BOUDJEMA, F., and ABATUT, J.L.: 'Sliding mode — a new way to control series resonant converter'. IEEE conference on *Industry electronics* 1990, pp. 938–943
15 BOUDJEMA, F., BOSCARDIN, M., BIDAN, P., MARPINHARD, J.C., VALENTIN, M., and ABATUT, J.L.: 'VSS approach to a full bridge buck converter used for AC sine voltage generation'. IEEE Conference on *Industry electronics* 1989, pp. 82–88
16 SARPTURK, S.Z., ISTEFANOPULOS, Y., and KAYNAK, O.: 'On stability of discrete-time sliding mode control system', *IEEE Trans.*, **AC-32**, (10), 1987, pp. 82–88
17 KO, J.H., HONG, S.S., ANN, T.Y., and YOUN, M.J.: 'Dynamic modeling and current control technique for quantum series resonant converter with non-periodic integral cycle mode', *Int. J. Electron.*, 1991, **71**, pp. 885–897

8 Appendix

8.1 Proof of lemma 1

By using the switching strategy of expr. 21 and 22, and the current slope equation (eqn. 18), the p-step prediction of the sliding surface in the discrete time domain is given by

$$[S(k+p) - S(k)]\ \mathrm{sgn}\ (S(k)) = \frac{1}{L_{eq}^{p}} \{pV_o(k) - \tfrac{1}{2}V_s(k)\}\ \mathrm{sgn}\ (S(k)) \quad (41)$$

where L_{eq}^{p} is the equivalence inductance with the $p-$ step prediction in eqn. 18. If $p \rightarrow N$ is taken, the modified sliding condition for the proposed buck-type converter can be obtained. The N-step prediction of the sliding surface has the negative value or the magnitude of the rectified line voltage in the $(k+N)$th time event $V_s(k+N)$ is larger than that of $2V_o(k)$ for $S(k) > 0$. Simi-

larly, the N-step prediction of the sliding surface has a positive value, or the magnitude of the rectified line voltage in the $(k + N)$th time event $V_s(k + N)$ is smaller than $2V_o(k)$ for $S(k) < 0$. Note that the integer N which implies finite sampling time is defined as

$$N = \min \{M, q\} \tag{42}$$

The positive integer q represents the minimum number of the finite sampling time when either positive current slope appears for $S(k) > 0$ or negative current slope is available for $S(k) < 0$ by the switching strategy as shown in Fig. 20. This is expressed mathematically as

$$q = \min \{i \mid [S(k + i) - S(k)] \text{ sgn } (S(k)) < 0\} \tag{43}$$

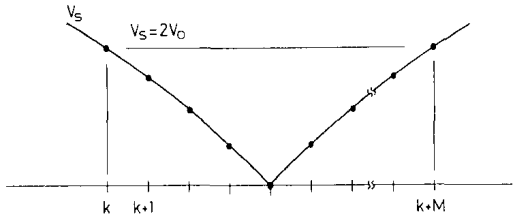

Fig. 20 *Typical waveform of rectified line voltage for buck operation*

The integer q depends on the switching strategy which makes the current slope have the desired polarity after q sampling time. On the other hand, since the line voltage is a sinusoidal time-varying voltage, the magnitude of the rectified line voltage in $(k + M)$th time event is larger than that of the rectified line voltage in the kth time event which is equal to $2V_o(k)$ for $S(k) > 0$ and smaller when $S(k) < 0$. From eqn. 41 positive current slope appears when $V_s(k + M) > 2V_o(k)$ for $S(k) > 0$ and negative current slope is available when $V_s(k + j) < 2V_o(k)$ for $S(k) < 0$ owing to the variation of $V_s(k)$ as shown in Fig. 21. This can be expressed mathematically as

$$M = \min \{j \mid [V_s(k) - V_s(k + j)] \text{ sgn } (S(k)) < 0\} \tag{44}$$

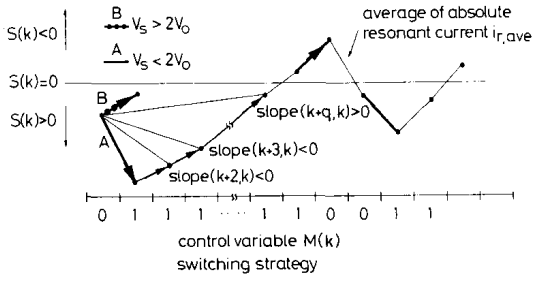

Fig. 21 *Typical waveform of $i_{r,ave}$ with respect to switching surface for buck operation*

After a modified quasisliding mode takes place, the sliding surface variation during N sampling time is bounded as follows:

$$|S(k + N) - S(k)| \leqslant \frac{1}{L_{eq}^N} \{NV_o(k) - M^*(k + 1)V_s(k)\}|_{max}$$

$$= \frac{1}{L_{eq}^N} NV_o(k) \tag{45}$$

This equation can be derived by setting $M^*(k + 1)$ to 0. Therefore a modified quasisliding motion for the proposed converter is not divergent.